J. Fluid Mech. (1987), *vol.* 183, *pp.* 219–234
Printed in Great Britain

Interface conditions for two-phase displacement in Hele-Shaw cells

By D. A. REINELT
Department of Mathematics, Southern Methodist University, Dallas, TX 75275, USA

(Received 13 January 1986 and in revised form 11 February 1987)

In displacing a viscous fluid from the gap between two closely spaced parallel plates, a thin film of the original fluid remains on the surface of each plate. Boundary conditions which connect the approximate equations in the region in front of the interface with the approximate solutions in the thin-film region are determined from local solutions of the equations in the vicinity of the interface edge. These interface conditions depend on both b/R (gap half-width/radius of curvature) and $\mu U_n/T$, where μ is the viscosity of the original fluid, U_n is the normal velocity of the interface edge, and T is the interfacial tension. These conditions are determined using perturbation method when $\mu U_n/T \ll 1$ and numerical methods when $\mu U_n/T$ is $O(1)$. Though previous theories have shown qualitative agreement with experiments, it is hoped that these new boundary conditions improve the quantitative agreement.

1. Introduction

When a less viscous fluid drives a more viscous fluid out of a Hele-Shaw cell, consisting of two closely spaced parallel plates, the interface between the two fluids is unstable. It was observed in experiments by Saffman & Taylor (1958) that the unstable interface forms into fingers of the less viscous fluid penetrating into the more viscous fluid. The shape of the interface between the two fluids depends on the capillary number, $Ca = \mu U/T$, where μ is the viscosity of the fluid that initially fills the Hele-Shaw cell, T is the surface tension, and U is a velocity characteristic of the moving interface. It also depends on the ratio of the distance between the two plates $2b$ to the width of the Hele-Shaw cell $2a$, where $\epsilon = b/a \ll 1$ (see figures 1 and 2). A third parameter, the ratio of the two viscosities, also effects the shape of the interface. For simplicity, we assume that the viscosity of the driving fluid can be neglected in comparison with the viscosity of the fluid that initially fills the gap between the plates. Using the methods discussed below, the results could be extended to include this third parameter. We also assume that the shape of the interface is symmetric about the mid-plane where $z = 0$, but not necessarily symmetric about the plane where $y = 0$.

For a Hele-Shaw cell of a given size, ϵ is fixed and the developing flow only depends on the capillary number. If Ca is not too large, it was observed by Saffman & Taylor (1985), Pitts (1980), Park & Homsy (1985), Tabeling, Zocchi & Libchaber (1987) and others that the flow develops into a single steady-state finger which moves through the cell with constant velocity U. For larger values of the capillary number, the interface branches into a number of different fingers and continues to evolve in time. The precise value of Ca at which there is a transition from a single steady-state finger to the more complicated pattern is unknown. Though figures 1 and 2 are drawn

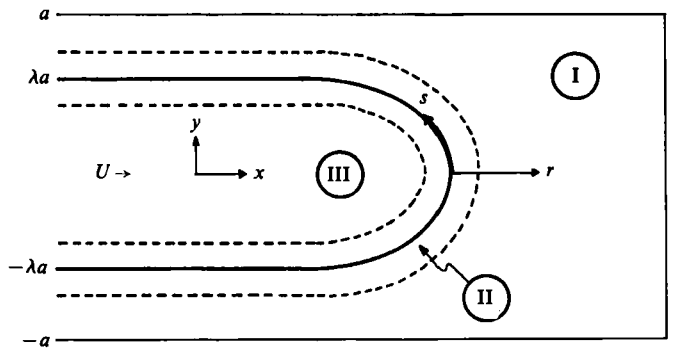

FIGURE 1. Top view of Hele-Shaw cell.

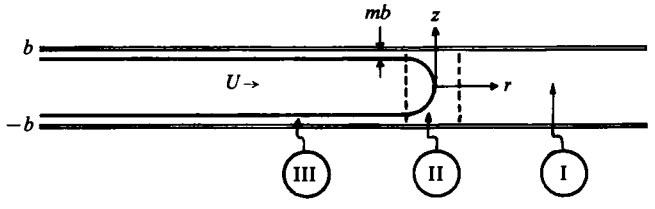

FIGURE 2. Side view of Hele-Shaw cell.

to represent the steady-state case, the boundary conditions developed below are also valid for the non-steady problem.

The main concern of investigators that have examined the above displacement problem is the shape of the leading edge of the interface, located in the mid-plane. Throughout this paper, the term lateral will refer to variations along this interface edge, while the term transverse will refer to variations in the plane perpendicular to the interface edge (see figure 2). The purpose of this paper is to determine approximate boundary conditions that take into account the flow in the transverse direction and its effect on the shape of the interface edge.

The solution of the complete three-dimensional Hele-Shaw displacement problem requires finding the shape of the interface and solving for the velocity $\boldsymbol{u} = (u, v, w)$ and pressure p in a domain bounded by the interface, the parallel plates at $z = \pm b$, and the sides of the cell at $y = \pm a$. The conservation equation and Stokes equation are

$$\nabla \cdot \boldsymbol{u} = 0, \tag{1}$$

$$\nabla p = \mu \nabla^2 \boldsymbol{u}. \tag{2}$$

The boundary condition $\boldsymbol{u} = 0$ is applied on $y = \pm a$ and $z = \pm b$. The interface conditions are

$$(\boldsymbol{u} - \boldsymbol{U}) \cdot \boldsymbol{n} = 0, \tag{3a}$$

$$\boldsymbol{t} \cdot \boldsymbol{\sigma} \cdot \boldsymbol{n} = 0, \tag{3b}$$

$$-\boldsymbol{n} \cdot \boldsymbol{\sigma} \cdot \boldsymbol{n} = p_0 - T\left(\frac{1}{R_1} + \frac{1}{R_2}\right), \tag{3c}$$

where $\boldsymbol{U}$ is the velocity of the interface, $\boldsymbol{\sigma}$ is the stress tensor, and $\boldsymbol{n}$ and $\boldsymbol{t}$ represent the unit normal and unit tangent vectors to the interface. The principal radii of

curvature of the interface are R_1 and R_2, the interfacial tension is T, and the constant pressure of the displacing fluid is p_0.

Since it is difficult to calculate the solution of the full three-dimensional problem, we divide the domain into three regions (see figures 1 and 2) and make approximations in each region based on $\epsilon = b/a \ll 1$. In Region I, away from the interface edge, the x- and y-variables are scaled by the length a and the z-variable by the length b. For $\epsilon \ll 1$, the velocity components are given by

$$u = \frac{p_x}{2\mu}(z^2 - b^2), \quad v = \frac{p_y}{2\mu}(z^2 - b^2), \quad w = 0, \tag{4a, b, c}$$

where the pressure p, to this approximation, is a function only of x and y. By averaging the velocity field across the gap between the plates, we get the well-known two-dimensional equations for the components of the mean velocity in the plane parallel to the plates (Lamb 1932),

$$\bar{u} = -\frac{b^2}{3\mu}p_x, \quad \bar{v} = -\frac{b^2}{3\mu}p_y, \tag{5a, b}$$

where b is the gap half-width.

In Region III, where there is a thin film of viscous fluid on the surface of each plate, x and y are scaled by a, and z is scaled by b. These are the same lengthscales as used in Region I. To this approximation, the velocity solution in the thin film is $\boldsymbol{u} = 0$, the pressure is p_0, and the shape of the interface is determined from the limiting values of the thickness mb (see figure 2). These values come from the outer limits of the solution in Region II. In the displacing fluid, the velocity close to Region II equals $\boldsymbol{U}$, the velocity of the interface edge. By averaging the velocity in the z-direction, we find that the mean velocity is $(1-m)\,\boldsymbol{U}$.

To complete the two-dimensional problem, two boundary conditions are needed to connect the solutions of Regions I and III. There is the kinematic condition given by

$$\bar{\boldsymbol{u}} \cdot \boldsymbol{n} = (1-m)\,(\boldsymbol{U} \cdot \boldsymbol{n}), \tag{6a}$$

where $\boldsymbol{n}$ is the normal to the interface edge and $\bar{\boldsymbol{u}} = (\bar{u}, \bar{v})$. There is also the dynamic condition relating the limits of the pressure on the two sides,

$$p - p_0 = \Delta p. \tag{6b}$$

The limiting values m and Δp are to be understood as outer limits in which the distance from the interface edge is small compared with a, but large compared with b. These values are determined from solutions of the appropriate equations in Region II. It should be noted that the width of Region II is $O(b)$; thus, the size of the region that is being replaced by boundary conditions (6a, b) is very small in comparison with the other two regions. For $\epsilon \ll 1$, we expect the limiting values of m and Δp to have the form

$$m = m^0\left(\frac{\mu U_n}{T}\right) + m^1\left(\frac{\mu U_n}{T}\right)\frac{b}{R} + \ldots \tag{7a}$$

and

$$\Delta p = \frac{T}{b}\left[\kappa^0\left(\frac{\mu U_n}{T}\right) + \kappa^1\left(\frac{\mu U_n}{T}\right)\frac{b}{R} + \ldots\right] \tag{7b}$$

where $U_n = \boldsymbol{U} \cdot \boldsymbol{n}$ and R is the radius of curvature of the interface edge. Since we are assuming that R is $O(a)$, the term b/R is $O(\epsilon)$. Once m and Δp are known, the shape

of the interface edge and the components of mean velocity can be found by solving (5*a*, *b*) with interface conditions (6*a*, *b*).

In the past, since the dependence of m and Δp on the capillary number was not known, the four functions m^0, m^1, κ^0, and κ^1 were assumed to be constant. Saffman & Taylor (1958) were able to find a closed-form solution, but were unable to determine the finger width λ (see figure 1) for the case in which both m^1 and κ^1 were equal to zero. For the case $\kappa^1 = -1$, McLean & Saffman (1981) and Vanden-Broeck (1983) calculated interface-edge profiles and widths λ for different values of the capillary number. The numerical and experimental finger profiles were in close agreement for fingers with the same width λ, but there was significant disagreement between the numerical and experimental results for the same value of the capillary number. In the hope of improving the agreement, the dependence of m and Δp on the capillary number is determined here.

This is accomplished by solving the appropriate equations in the transverse direction. At any point along the interface edge, the shape of the interface in the plane perpendicular to the interface edge depends only on the lateral curvature (b/R) and normal velocity ($\mu U_n/T$) at that point. Once these solutions are determined for different values of b/R and $\mu U_n/T$, the functions m and Δp can be found. In fact, given a moving interface edge of arbitrary shape, these solutions can be used to determine the entire shape of the interface in Region II.

Since the solution in the plane perpendicular to the interface edge depends only on b/R and $\mu U_n/T$, we examine the simpler problem in which the interface edge is an expanding circle of radius R. This axisymmetric problem is solved in two ways. First, using singular perturbation methods and matched asymptotic expansions, the four functions in (7*a*, *b*) are determined for small values of the capillary number Ca. These results are closely related to the work of Bretherton (1961), which solved the problem in which the interface edge is straight ($b/R = 0$), and the more recent work of Park & Homsy (1984), which considered the problem in which small lateral variations from a straight interface edge are allowed. Unfortunately, in all three problems, m and Δp can only be determined up to $O(Ca^{\frac{2}{3}})$. This means that the expansions are only valid for very small values of the capillary number. Appropriate equations for the $O(Ca)$-terms can be found, but these partial differential equations would have to be solved numerically.

Secondly, the entire axisymmetric problem is solved numerically for different values of b/R and Ca. This is done by beginning with an approximate shape of the interface, covering the resulting domain with a composite mesh, and using finite-difference methods to find the solution. The correct interface is then determined using an iteration method. By combining the perturbation solution, valid for small values of Ca, with the numerical solution, the functions m and Δp are determined.

In §5, the appropriate equations in Region II are derived directly from the three-dimensional Hele-Shaw equations (1), (2) and (3). This is done by introducing an orthogonal curvilinear coordinate system in Region II based on the arbitrary shape of the interface edge and by introducing dimensionless variables which take into account the different lengthscales. The resulting equations verify the correctness of the assumed form of m and Δp in (7*a*, *b*) and the axisymmetric equations discussed above.

2. Formulation of the axisymmetric problem

We consider the problem in which the driving fluid is injected at the origin of the coordinate system described in §1. We assume that the interface edge expands circularly (no lateral variations) with velocity U and that the radius R of the interface edge is much larger than the gap half-width b. Our main interest concerns the interface shape and the pressure for different values of the capillary number $Ca = \mu U/T$ and lateral curvature $\delta = b/R \ll 1$.

The axisymmetric conservation equation and Stokes equations for the viscous fluid are

$$\tilde{u}_{\tilde{r}} + \frac{\tilde{u}}{\tilde{r}} + \tilde{w}_{\tilde{z}} = 0, \tag{8a}$$

$$\tilde{p}_{\tilde{r}} = \mu\left[\nabla^2\tilde{u} - \frac{\tilde{u}}{\tilde{r}^2}\right], \tag{8b}$$

$$\tilde{p}_{\tilde{z}} = \mu[\nabla^2\tilde{w}], \tag{8c}$$

where the tilde denotes the physical variables and μ is the viscosity. We introduce dimensionless variables and a local reference frame centred at the edge of the interface by the following change of variables:

$$\left.\begin{aligned} r = \frac{\tilde{r}-R}{b}, \quad z = \frac{\tilde{z}}{b}, \quad h = \frac{\tilde{h}}{b}, \\ u = \frac{\tilde{u}-U}{U}, \quad w = \frac{\tilde{w}}{U}, \quad p = \frac{\tilde{p}-\tilde{p}_0}{T/b}. \end{aligned}\right\} \tag{9}$$

Here, $\tilde{p}_0$ is the constant pressure of the driving fluid and T is the interfacial tension. The scaling for the pressure comes from balancing the pressure and curvature terms in the normal-stress boundary condition (12c) given below. The function $z = h(r)$ gives the shape of the interface in the (r, z)-plane. The dimensionless equations for (8a, b, c) are

$$u_r + \frac{\delta}{1+\delta r}(u+1) + w_z = 0, \tag{10a}$$

$$p_r = Ca\left[\nabla^2 u - \frac{\delta^2}{(1+\delta r)^2}(u+1)\right], \tag{10b}$$

$$p_z = Ca[\nabla^2 w], \tag{10c}$$

where

$$\nabla^2 w = w_{rr} + \frac{\delta}{1+\delta r} w_r + w_{zz}.$$

The boundary conditions on the plates $z = \pm 1$ are

$$u = -1, \quad w = 0. \tag{11a, b}$$

Since the interface is symmetric about the mid-plane, it is sufficient to determine the solution for $z \geqslant 0$. The interface conditions to be satisfied on $z = h(r) \geqslant 0$ are

$$h_r u - w = 0, \tag{12a}$$

$$(1-h_r^2)(u_z + w_r) - 2h_r(u_r - w_z) = 0, \tag{12b}$$

$$p - 2Ca\left[\frac{h_r^2 u_r - h_r(u_z + w_r) + w_z}{1+h_r^2}\right] = \frac{h_{rr}}{(1+h_r^2)^{\frac{3}{2}}} + \frac{\delta h_r}{(1+\delta r)(1+h_r^2)^{\frac{1}{2}}}, \tag{12c}$$

where the terms on the right-hand side of (12*c*) are the principal curvatures multiplied by a negative sign. These equations must now be solved for different values of the parameters Ca and δ.

In the more general displacement problem, we also introduce a coordinate r in Region II that is normal to the interface edge and scaled by the lengthscale b (see §5). In both problems, values of the scaled variable r that are $O(1)$ correspond to values of the physical variable that are a distance $O(b)$ away from the interface edge. This means that when $\epsilon \ll 1$ the outer limits of the solution in Region II, which match onto the solutions in Regions I and III, correspond to the limits $r \to \infty$ and $r \to -\infty$. This also means that the boundary conditions at the sides of the cell do not enter into the equations that must be solved in Region II.

The thickness m and pressure jump Δp in boundary conditions (6*a*, *b*) are determined from solutions of the axisymmetric problem by examining these limits. As $r \to -\infty$, the interface approaches a constant value ($h_z \to 0$); thus, the thickness of the thin-film region is

$$m(Ca, \delta) = \lim_{r \to -\infty} [1 - h(r; Ca, \delta)], \tag{13}$$

where we have indicated that the shape of the interface depends on both parameters. The limiting value of the velocity components and pressure are

$$u \to -1, \quad w \to 0, \quad p \to 0. \tag{14a, b, c}$$

These asymptotic results are used in the numerical solution of the problem.

As $r \to \infty$, the solution components are

$$u \to -1 + \tfrac{3}{2} B \frac{1 - z^2}{1 + \delta r}, \quad w \to 0, \tag{15a, b}$$

and the pressure is

$$p \to -\frac{3BCa}{\delta} \log(1 + \delta r) + \kappa(Ca, \delta). \tag{15c}$$

The constant B is related to the flow as $r \to -\infty$ and is defined in §4. The constant κ is determined when the axisymmetric problem is solved numerically. In the Hele-Shaw displacement problem, we replace Region II by an appropriate pressure-jump condition at the interface edge ($r = 0$). This value is determined by the difference of the two asymptotic results (14*c*), (15*c*) evaluated at $r = 0$ and is equal to $\kappa(Ca, \delta)$.

3. Perturbation solution

To determine the perturbation solution of the axisymmetric problem discussed in §2, we assume that both parameters are small;

$$Ca = \frac{\mu U}{T} \ll 1, \quad \delta = \frac{b}{R} \ll 1.$$

Bretherton (1961) solved this problem for the case $\delta = 0$, which is equivalent to a straight interface in the lateral direction. Park & Homsy (1984) made significant progress in the case $\delta \ll 1$ by considering the problem in which small lateral variations along a straight interface edge are allowed. In the axisymmetric problem, there are no lateral variations along the interface and the radius of curvature of the interface edge is equal to R. Though the equations and solutions in the Park & Homsy problem

and the axisymmetric problem are similar, there are some differences which can best be illustrated by examining the more general perturbation problem in which the interface edge has an arbitrary shape (see §6).

It is known from the work of Bretherton that this type of problem is a singular perturbation problem in the capillary number Ca and that the expansion involves powers of $Ca^{\frac{1}{3}}$. The axisymmetric problem is a regular perturbation problem in δ and can be expanded in powers of δ. The perturbation solution is composed of an outer expansion, valid away from the thin-film region, and an inner expansion, valid near the thin-film region. These two expansions are matched in an overlap region using the techniques of matched asymptotic expansions.

In the outer region, away from the thin-film region, (10), (11) and (12) are valid. We expand the pressure and shape of the interface in the outer region by setting

$$p = p^0 + \delta p^1 + Ca^{\frac{2}{3}} p^2 + \delta Ca^{\frac{2}{3}} p^3 + \ldots \tag{16a}$$

and

$$h = h^0 + \delta h^1 + Ca^{\frac{2}{3}} h^2 + \delta Ca^{\frac{2}{3}} h^3 + \ldots . \tag{16b}$$

From the work of Bretherton, it is known that the $Ca^{\frac{1}{3}}$ term is not necessary in the outer expansion. If we include these terms, we find that they are equal to zero when the matching is completed. For simplicity, these terms have not been included in the expansion.

When the pressure expansion (16a) is substituted into (10b, c), we discover that all four terms in (16a) are constant and that the velocity does not enter into the problem until we reach pressure terms of $O(Ca)$. From (12c), the four terms in the expansion of h given in (16b) must satisfy

$$p = \frac{h_{rr}}{(1+h_r^2)^{\frac{3}{2}}} + \frac{\delta h_r}{(1+h_r^2)^{\frac{1}{2}}}. \tag{17}$$

Terms in (12c) of $O(Ca)$ and $O(\delta^2)$ do not enter into the problem at this order and have been dropped. To find the appropriate second-order ordinary differential equation for each term in the expansion of h, we substitute both expansions (16a, b) into (17), expand the right-hand side in powers of $Ca^{\frac{2}{3}}$ and δ, and match like powers on each side of the equation. The constants of integration are chosen such that h_r is integrable as $r \to 0$ and $h(0) = 0$.

The leading-order equation to solve is

$$p^0 = \frac{h^0_{rr}}{(1+h_r^{02})^{\frac{3}{2}}}. \tag{18}$$

When the capillary number is zero, the thickness of the thin film is zero and the gap is completely filled by the displacing fluid. We assume that the interface approaches the upper plate tangentially at some point $r = l = l^0 + \delta l^1 + \ldots, z = 1$ (i.e. the contact angle is zero). Under these conditions, the solution of (18) is a semicircle with radius equal to 1,

$$h^0 = [1-(r+1)^2]^{\frac{1}{2}} \tag{19}$$

with

$$p^0 = -1, \quad l^0 = -1. \tag{20a, b}$$

The $O(\delta)$-equation is

$$p^1 = \frac{h^1_{rr}}{(1+h_r^{02})^{\frac{3}{2}}} - \frac{3h^0_r h^0_{rr} h^1_r}{(1+h_r^{02})^{\frac{5}{2}}} + \frac{h^0_r}{(1+h_r^{02})^{\frac{1}{2}}}, \tag{21}$$

which has the solution

$$h^1 = -\frac{p^1 r}{[1-(r+1)^2]^{\frac{1}{2}}} - \tfrac{1}{2}\sin^{-1}(r+1) + \tfrac{1}{4}\pi. \tag{22}$$

To determine p^1 and l^1, we evaluate h and h_r at $r = l$,

$$h^0(l)+\delta h^1(l) = 1+\delta(p^1+\tfrac{1}{4}\pi)+O(\delta^2), \tag{23a}$$

$$h^0_r(l)+\delta h^1_r(l) = \delta(-l^1-p^1-\tfrac{1}{2})+O(\delta^2). \tag{23b}$$

Since the interface intersects the plate tangentially at $r = l$, we get

$$p^1 = -\tfrac{1}{4}\pi, \quad l^1 = \tfrac{1}{4}\pi-\tfrac{1}{2}. \tag{24a, b}$$

This value of p^1 was first determined by Park & Homsy (1984).

To determine the dependence of the solution on the capillary number, we solve the $O(Ca^{\frac{2}{3}})$-equation given by

$$p^2 = \frac{h^2_{rr}}{(1+h^{02}_r)^{\frac{3}{2}}}-\frac{3h^0_r h^0_{rr} h^2_r}{(1+h^{02}_r)^{\frac{5}{2}}}. \tag{25}$$

Its solution is

$$h^2 = -\frac{p^2 r}{[1-(r+1)^2]^{\frac{1}{2}}}. \tag{26}$$

Finally, the $O(\delta Ca^{\frac{2}{3}})$-equation is

$$p^3 = \frac{h^3_{rr}}{(1+h^{02}_r)^{\frac{3}{2}}}-\frac{3h^0_{rr}(h^0_r h^3_r+h^1_r h^2_r)}{(1+h^{02}_r)^{\frac{3}{2}}}-\frac{3h^0_r(h^1_r h^2_{rr}+h^2_r h^1_{rr})}{(1+h^{02}_r)^{\frac{5}{2}}} + \frac{15h^{02}_r h^0_{rr} h^1_r h^2_r}{(1+h^{02}_r)^{\frac{7}{2}}}+\frac{h^2_r}{(1+h^{02}_r)^{\frac{1}{2}}}-\frac{h^{02}_r h^2_r}{(1+h^{02}_r)^{\frac{3}{2}}}, \tag{27}$$

and the solution is

$$h^3 = -\frac{p^3 r}{[1-(r+1)^2]^{\frac{1}{2}}}-\frac{p^1 p^2 r(2r+3)}{(r+2)[1-(r+1)^2]^{\frac{1}{2}}}-p^2\left[\sin^{-1}(r+1)-\frac{r}{2[1-(r+1)^2]^{\frac{1}{2}}}-\tfrac{1}{2}\pi\right]. \tag{28}$$

The values of p^2 and p^3 are determined in the matching process.

We now examine the transition or inner region which connects the solution in the outer region with the thin film of constant thickness. The transition region is centred at the point $r = l$ and $z = 1$ where the interface determined in the outer expansion meets the upper plate. We introduce local variables at this point by the following change of variables:

$$\left.\begin{aligned} \bar{r} = \frac{r-l}{Ca^{\frac{1}{3}}}, \quad \bar{z} = \frac{z-1}{Ca^{\frac{1}{3}}}, \quad \bar{h} = \frac{h-1}{Ca^{\frac{2}{3}}}, \\ \bar{u} = u, \quad \bar{w} = \frac{w}{Ca^{\frac{1}{3}}}, \quad \bar{p} = p. \end{aligned}\right\} \tag{29}$$

These scalings give the lubrication approximation in the transition region. The appropriate transition equations are found by substituting the local variables (29) into (10), (11) and (12). The velocity and pressure field can be explicitly determined in terms of the interface shape. The leading-order shape of the interface satisfies the ordinary differential equation

$$\bar{h}_{\bar{r}\bar{r}\bar{r}} = -\frac{3(\bar{h}+\bar{m})}{\bar{h}^3}, \tag{30}$$

where $\bar{h}\to-\bar{m}$ as $\bar{r}\to-\infty$ and $m = Ca^{\frac{2}{3}}\bar{m}$ is the constant thickness of the thin-film

region. See Bretherton (1961) for the derivation of this equation. The above equation is integrated numerically, beginning with the asymptotic solution as $\bar{r} \to -\infty$,

$$\bar{h} \sim -\bar{m} - \bar{m} \exp\left[\frac{3^{\frac{1}{2}}}{\bar{m}}(\bar{r}+\bar{r}_0)\right] + \ldots, \tag{31}$$

in order to determine the constants $\bar{a}$, $\bar{b}$, and $\bar{c}$ in the asymptotic solution as $\bar{r} \to \infty$,

$$\bar{h} \sim \frac{\bar{a}}{\bar{m}}(\bar{r}+\bar{r}_0)^2 + \bar{b}(\bar{r}+\bar{r}_0) + \bar{c}\bar{m} + \ldots. \tag{32}$$

The values of these constants are

$$\bar{a} = -0.6687, \quad \bar{b} = -0.014, \quad \bar{c} = -2.84.$$

The unknown constants $\bar{m}$ and $\bar{r}_0$ are scaled out of the equation before the integration is done. To facilitate matching with the outer expansion, we rewrite (32) in terms of outer variables by using (29):

$$h \sim 1 + \frac{\bar{a}}{\bar{m}}(r-l)^2 + Ca^{\frac{1}{3}}\left(\bar{c} - \frac{\bar{b}^2}{4\bar{a}}\right)\bar{m} + O(Ca), \tag{33}$$

where the translation constant r_0 was chosen to eliminate the $O(Ca^{\frac{1}{3}})$-term which cannot be matched in the outer expansion,

$$\bar{r}_0 = -\frac{\bar{b}\bar{m}}{2\bar{a}}.$$

It is important to note that the leading-order equations in the transition region, found by setting $Ca = 0$, are independent of δ. This means that Bretherton's result is also valid for non-zero δ and the unknown constant $\bar{m}$ can depend on δ. By substituting

$$\bar{m} = \bar{m}^0 + \delta\bar{m}^1 + \ldots, \quad l = l^0 + \delta l^1 + \ldots = -1 + \delta(\tfrac{1}{4}\pi - \tfrac{1}{2}) + \ldots$$

into (33) and expanding in powers of δ, we get the following expression for h:

$$h \sim 1 + \frac{\bar{a}}{\bar{m}^0}(r+1)^2 + \delta\left(\frac{-2\bar{a}}{\bar{m}^0}\right)\left[(\tfrac{1}{4}\pi - \tfrac{1}{2})(r+1) + \frac{\bar{m}^1}{2\bar{m}^0}(r+1)^2\right] + Ca^{\frac{1}{3}}\left(\bar{c} - \frac{\bar{b}^2}{4\bar{a}}\right)\bar{m}^0 + \delta Ca^{\frac{1}{3}}\left(\bar{c} - \frac{\bar{b}^2}{4\bar{a}}\right)\bar{m}^1 + \ldots. \tag{34}$$

The constants $\bar{m}_0$ and $\bar{m}_1$ are determined by matching the asymptotic solution in the transition region as $\bar{r} \to \infty$ given in (34) with the asymptotic solution in the outer region as $r \to -1$.

The shape of the interface in the outer region is $h \sim h^0 + \delta h^1 + Ca^{\frac{1}{3}}h^2 + \delta Ca^{\frac{1}{3}}h^3 + \ldots$ where the four terms are given in (19), (22), (26) and (28). These terms are expanded in powers of $r+1$, which gives

$$h \sim [1 - \tfrac{1}{2}(r+1)^2 + \ldots] + \delta[(\tfrac{1}{4}\pi - \tfrac{1}{2})(r+1) - \tfrac{1}{8}\pi(r+1)^2 + \ldots] + Ca^{\frac{1}{3}}[p^2 + \ldots] + \delta Ca^{\frac{1}{3}}[p^3 + p^1p^2 + (\tfrac{1}{2}\pi - \tfrac{1}{2})p^2 + \ldots] + \ldots. \tag{35}$$

Matching the $O(1)$- and $O(\delta)$-terms in (34) and (35) determines $\bar{m}^0$ and $\bar{m}^1$:

$$\bar{m}^0 = -2\bar{a} = 1.3375, \quad \bar{m}^1 = -\tfrac{1}{4}\pi\bar{m}^0.$$

Matching the next two terms determines p^2 and p^3:

$$p^2 = -3.80, \quad p^3 = 4.07.$$

Therefore, the perturbation solutions for the film thickness and pressure jump (7*a*, *b*) discussed in §1 are

$$m = (1.3375Ca^{\frac{2}{3}} + \ldots) + (-1.3375\tfrac{1}{4}\pi Ca^{\frac{2}{3}} + \ldots)\frac{b}{R} + \ldots, \tag{36a}$$

and

$$\kappa = (-1 - 3.80Ca^{\frac{2}{3}} + \ldots) + (-\tfrac{1}{4}\pi + 4.07Ca^{\frac{2}{3}} + \ldots)\frac{b}{R} + \ldots. \tag{36b}$$

The next term in each of the quantities in parentheses is $O(Ca)$, so these expressions will only be valid for very small values of the capillary number. To determine higher-order terms in the expansion requires calculating both the velocity and pressure in the outer region. The resulting sets of partial differential equations could be solved numerically, but it makes more sense to numerically solve the original axisymmetric problem (10)–(12) for a larger range of capillary numbers instead.

4. Numerical solution

To solve (10)–(12) numerically, we introduce the stream function ψ given by

$$u = \frac{1}{1+\delta r}\psi_z - 1, \quad w = -\frac{1}{1+\delta r}\psi_r \tag{37a, b}$$

and the vorticity ω given by

$$\omega = w_r - u_z. \tag{37c}$$

The new versions of (10*a*, *b*, *c*) are

$$\psi_{rr} + \psi_{zz} - \frac{\delta}{1+\delta r}\psi_r = -(1+\delta r)\,\omega, \tag{38a}$$

$$\omega_{rr} + \omega_{zz} + \frac{\delta}{1+\delta r}\omega_r - \frac{\delta^2}{(1+\delta r)^2}\omega = 0, \tag{38b}$$

$$p_{rr} + p_{zz} + \frac{\delta}{1+\delta r}p_r = 0. \tag{38c}$$

The pressure equation is solved independently of the other two equations.

If we substitute (37*a*, *b*) into the first interface condition (12*a*), we get

$$\psi_r + h_r\psi_z = (1+\delta r)\,h_r.$$

This expression can be integrated to give ψ on the interface:

$$\psi = h + \delta\int_0^r r h_r\,\mathrm{d}r. \tag{39a}$$

The second interface condition (12*b*) can be rewritten as

$$\omega + \frac{2h_{rr}}{1+h_r^2}\left(1 - \frac{1}{1+\delta r}\psi_z\right) = 0, \tag{39b}$$

using (37*a*, *b*, *c*) and derivatives of (39*a*). The third interface condition (12*c*),

$$p - 2Ca\left[\frac{h_r^2 u_r - h_r(u_z + w_r) + w_z}{1+h_r^2}\right] = \frac{h_{rr}}{(1+h_r^2)^{\frac{3}{2}}} + \frac{\delta h_r}{(1+\delta r)\,(1+h_r^2)^{\frac{1}{2}}}, \tag{39c}$$

is written in terms of ψ by replacing the velocity terms in brackets with appropriate derivatives of (37a, b).

Since we are assuming that the interface is symmeric about the mid-plane, the boundary conditions on $z = 0$ are

$$\psi = 0, \quad \omega = 0. \tag{40a, b}$$

On the top plate $z = 1$, we have

$$\psi = B, \quad \psi_z = 0, \tag{41a, b}$$

where the value of the constant B is determined by letting $r \to -\infty$ in the integral given in (39a). The derivative h_r decays exponentially as $r \to -\infty$; thus, we get an accurate value for B by integrating to some appropriate finite value $r_{\min}$.

The asymptotic solutions for ψ and ω as $r \to \pm\infty$ are

$$\psi \to B, \quad \omega \to 0 \quad \text{as } r \to -\infty \tag{42a, b}$$

and

$$\psi \to \tfrac{3}{2}B(z - \tfrac{1}{3}z^3), \quad \omega \to \frac{3Bz}{1+\delta r} \quad \text{as } r \to \infty. \tag{43a, b}$$

Equations (38)–(41) are solved numerically on a finite domain by applying these asymptotic solutions at the finite values $r_{\min}$ and $r_{\max}$. We choose the size of the domain to be large enough such that the thickness m and pressure jump κ would not change if the domain were even larger. Typical values are $r_{\min} = -3.0$ and $r_{\max} = 2.0$.

To determine the numerical solution for given values of Ca and δ, we begin with an approximate shape for the interface profile. If the value of Ca is very small, we can use the perturbation solution; otherwise, we increase the value of Ca in increments using the interface shape calculated at the previous value. Since the shape of the interface is fixed, it is necessary to drop one of the interface conditions (39a, b, c). Either the normal-velocity condition (39a) or normal-stress condition (39c) is usually dropped. In order to calculate the pressure and velocity fields separately, we eliminate condition (39c). The remaining equations are then solved on a domain bounded by the approximate shape of the interface, the plate $z = 1$ and the mid-plane. This domain is covered by a composite mesh composed of a curvilinear grid which follows the curved interface, and a rectilinear grid parallel to the mid-plane and parallel plates. A typical curvilinear grid has 50 points along the interface and 7 points perpendicular to the interface. A typical rectilinear grid has 45 points in the x-direction and 35 points in the y-direction. The curvilinear grid is constructed using cubic-spline interpolation. This method of grid generation can be easily applied to problems with very complex domains. It is also flexible enough to allow for stretching in the grids so that the number of grid points is greatest in regions where they are needed most. Numerical codes are being developed by other researchers that will automatically generate the different grids for a region of arbitrary shape. Interpolation equations are used to connect the solutions on the overlapping grids.

After the velocity field has been determined using finite-difference methods, we solve (38c) on the same composite mesh to determine the pressure. The resulting solutions are substituted into the normal-stress condition (39c). The shape of the interface is then altered, and the procedure is repeated until this last interface condition is satisfied within a given tolerance. In practice, it takes about three or four iterations. For complete details of the numerical procedure discussed above, see Reinelt & Saffman (1985).

For each value of the capillary number shown in figures 3 and 4, ranging from

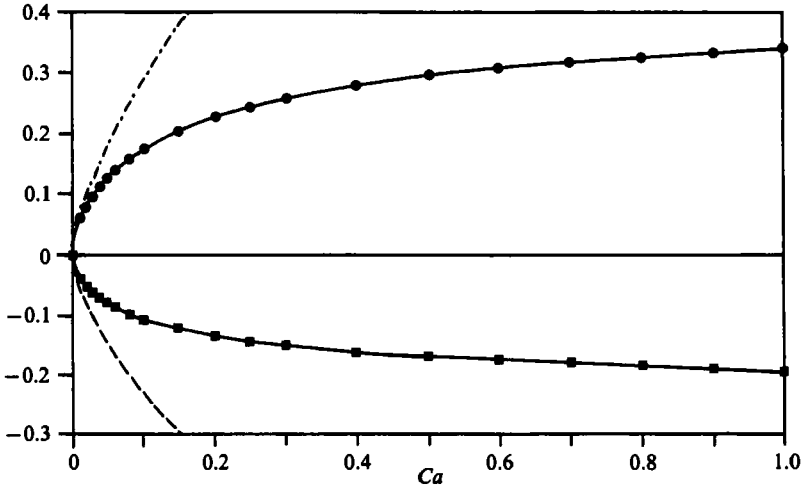

FIGURE 3. Coefficients for the thickness of the thin film m versus the capillary number. —●—, numerical result for m^0; —·—, perturbation result for m^0; —■—, numerical result for m^1; – – – –, perturbation result for m^1.

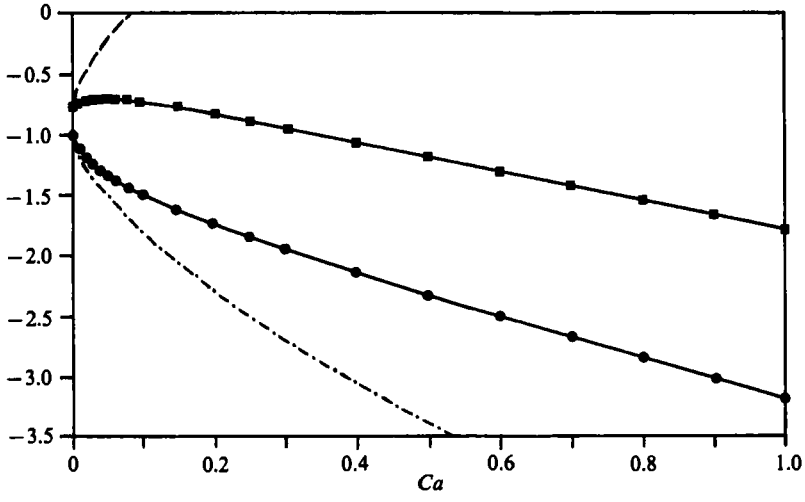

FIGURE 4. Coefficients for the pressure jump Δp versus the capillary number. —●—, numerical result for κ^0; —·—, perturbation result for κ^0; —■—, numerical result for κ^1; – – – –, perturbation result for κ^1.

$Ca = 0.01$ to 1.0, the solution is first calculated for $\delta = 0$. From these solutions, the functions m^0 and κ^0 are determined. Next, we set $\delta = 0.01$ and recalculate the solution for each value of the capillary number. The functions m^1 and κ^1 in (7a, b) are then found using both the $\delta = 0$ and $\delta = 0.01$ solutions. Finally, we calculate the solutions at the value $\delta = 0.02$ (and in a number of cases additional values), in order to verify that both m^1 and κ^1 are sufficiently accurate. An alternative approach involves linearizing in δ and solving the resulting set of partial differential equations. This requires making a number of substantial changes in the numerical code, primarily

due to the interface conditions which must be evaluated on the perturbed interface and then expanded in Taylor series about the unperturbed interface. The first approach was adopted because it was much simpler to implement.

It is clear from figures 3 and 4 that the perturbation solutions (36*a*, *b*) are only valid for very small values of the capillary number. This is to be expected because the next term in each of the expansions is $O(Ca)$; thus, the relative error in each expression is $O(Ca^{\frac{1}{2}})$. This means that even if Ca is as small as 1×10^{-3}, the relative error is $O(10\,\%)$ and, depending on the constants, could easily be in the neighbourhood of 30–40 %. All of the differences between the numerical and perturbation results in figures 3 and 4 are within these error estimates. (The numerical methods discussed above have also been applied to an axisymmetric finger propagating in a capillary tube of circular cross-section by Reinelt & Saffman (1985). Here, the numerical results were in excellent agreement with the experimental results of Taylor (1961) for different values of the capillary number.)

5. Derivation of the Region II equations

In Region I, away from the interface edge, the x- and y-variables were scaled by a, and the z-variable was scaled by b. In Region II, near the interface edge, these scalings are no longer valid. In this region, we replace the x- and y-coordinates by a coordinate r which varies in the direction perpendicular to the interface edge, and a coordinate s which varies in the direction tangential to the interface edge (see figures 1 and 2). The appropriate lengthscale in both the perpendicular direction and the z-direction is now b, while the lengthscale in the tangential direction is a. The equations for Region II are determined by transforming the general Hele-Shaw displacement equations (1)–(3) into the new r, s, and z orthogonal curvilinear coordinate system. To determine the relative importance of each term in the equations, we introduce dimensionless variables that take into account the different lengthscales.

The curvilinear coordinate system discussed above is based on the shape of the interface edge and moves with the interface. Let the shape of the interface edge $(r, z = 0)$ be given by

$$x = a\hat{x}(s,t), \quad y = a\hat{y}(s,t), \tag{44}$$

where $\hat{x}$ and $\hat{y}$ are dimensionless functions and s is a dimensionless arclength variable satisfying

$$\hat{x}_s^2 + \hat{y}_s^2 = 1.$$

The curvature of the interface edge $\hat{C}$ is an important parameter in Region II. It is related to $\hat{x}$ and $\hat{y}$ by

$$\hat{C}(s,t) = \frac{1}{\hat{R}} = \hat{x}_s \hat{y}_{ss} - \hat{y}_s \hat{x}_{ss}, \tag{45}$$

where $R = a\hat{R}$. The transformation between the two coordinate systems is

$$x = a\hat{x} + br\hat{y}_s, \quad y = a\hat{y} - br\hat{x}_s, \quad z = b\hat{z}, \tag{46}$$

where the lengthscales were introduced to make the variables on the right-hand side dimensionless. The coordinate r varies in the direction $(\hat{y}_s, -\hat{x}_s, 0)$, the normal to the interface edge. The tangent to the interface edge is $(\hat{x}_s, \hat{y}_s, 0)$. From the transformation

equations (46), distance in physical variables is related to distance in the new coordinate system through the expression

$$dx^2+dy^2+dz^2 = a^2[\epsilon^2\,dr^2+(1+\epsilon r\hat{C})^2\,ds^2+\epsilon^2\,d\hat{z}^2]. \tag{47}$$

The coefficients of the differentials on the right-hand side are used in the derivation of the transformed Hele-Shaw equations. For convenience, the hat is dropped from $\hat{z}$ in the rest of this section.

The dimensionless velocities $\hat{u}$, $\hat{v}$ and $\hat{w}$ in the r-, s- and z-directions respectively are

$$\hat{u} = \frac{(u,v,w)\cdot(\hat{y}_s,-\hat{x}_s,0)-U_n}{U_n}, \quad \hat{v} = \frac{(u,v,w)\cdot(\hat{x}_s,\hat{y}_s,0)}{\epsilon U_n}, \quad \hat{w} = \frac{w}{U_n}, \tag{48}$$

and the dimensionless pressure is

$$\hat{p} = \frac{p-p_0}{T/b},$$

where $U_n(s,t)$ is the normal velocity of the interface edge and $\epsilon = b/a \ll 1$. It is important to note that the normal velocity $\hat{u}$ is $O(U_n)$, but that the tangential velocity $\hat{v}$ is only $O(\epsilon U_n)$. The correct scaling for the tangential velocity can be determined by balancing the derivative of $\hat{p}$ with respect to s in Stokes equation (51b) with the most important term on the right-hand side. It can also be determined by rewriting (5a, b) of Region I in terms of the new coordinate system so that they become

$$\hat{u} = -\frac{\hat{p}_r}{3Ca}-1, \quad \hat{v} = -\frac{\hat{p}_s}{3Ca(1+\epsilon r\hat{C})}. \tag{49a, b}$$

In the transformed equations, derivatives with respect to s are multiplied by the factor $\epsilon/(1+\epsilon r\hat{C})$ when compared with derivatives with respect to either r or z (see (47)). This means that the tangential velocity must be scaled by ϵU_n in order to get the appropriate balance given in (49b).

To find the appropriate equations to solve in Region II, we rewrite the Hele-Shaw displacement equations (1)–(3) in terms of our new coordinate system. This was accomplished using appendix 2 in Batchelor (1967). The new conservation equation which replaces (1) is

$$\hat{u}_r+\frac{\epsilon\hat{C}}{1+\epsilon r\hat{C}}(\hat{u}+1)+\frac{\epsilon^2}{1+\epsilon r\hat{C}}\hat{v}_s+\hat{w}_z = 0. \tag{50}$$

Notice that the tangential velocity is not important in the conservation equation until we reach terms of $O(\epsilon^2)$. The components of Stokes equation (2) in the new coordinate system are

$$\hat{p}_r = Ca\left[\nabla^2\hat{u}-\frac{\epsilon^2\hat{C}^2}{(1+\epsilon r\hat{C})^2}(\hat{u}+1)-\frac{2\epsilon^3\hat{C}}{(1+\epsilon r\hat{C})^2}\hat{v}_s-\frac{\epsilon^3\hat{C}_s}{(1+\epsilon r\hat{C})^3}\hat{v}\right], \tag{51a}$$

$$\frac{1}{1+\epsilon r\hat{C}}\hat{p}_s = Ca\left[\nabla^2\hat{v}-\frac{\epsilon^2\hat{C}^2}{(1+\epsilon r\hat{C})^2}\hat{v}+\frac{2\epsilon\hat{C}}{(1+\epsilon r\hat{C})^2}\hat{u}_s+\frac{\epsilon\hat{C}_s}{(1+\epsilon r\hat{C})^3}(\hat{u}+1)\right], \tag{51b}$$

$$\hat{p}_z = Ca[\nabla^2\hat{w}], \tag{51c}$$

where

$$\nabla^2\hat{u} = \hat{u}_{rr}+\frac{\epsilon\hat{C}}{1+\epsilon r\hat{C}}\hat{u}_r+\frac{\epsilon}{1+\epsilon r\hat{C}}\left(\frac{\epsilon}{1+\epsilon r\hat{C}}\hat{u}_s\right)_s+\hat{u}_{zz}.$$

The capillary number in the above equations is based on the normal velocity of the interface edge, $Ca = \mu U_n/T$. Interface conditions (3a, b, c) can also be transformed

into the new coordinate system using (46) and (48), where the shape of the interface is $z = h(r, s)$. These conditions involve many terms and are not written out here.

Since we are only interested in the solution in Region II up to $O(\epsilon)$, we drop all $O(\epsilon^2)$-terms and other higher-order terms. The new simpler versions of (50) and (51) are

$$\hat{u}_r + \epsilon\hat{C}(\hat{u}+1) + \hat{w}_z = 0, \tag{52}$$

$$\hat{p}_r = Ca[\hat{u}_{rr} + \epsilon\hat{C}\hat{u}_r + \hat{u}_{zz}], \tag{53a}$$

$$\hat{p}_s = Ca(1+\epsilon r\hat{C})[\hat{v}_{rr} + \epsilon\hat{C}\hat{v}_r + \hat{v}_{zz} + 2\epsilon\hat{C}\hat{u}_s + \epsilon\hat{C}_s(\hat{u}+1)], \tag{53b}$$

$$\hat{p}_z = Ca[\hat{w}_{rr} + \epsilon\hat{C}\hat{w}_r + \hat{w}_{zz}]. \tag{53c}$$

The $\hat{u}$- and $\hat{w}$-equations (52), (53*a*) and (53*c*) and the appropriate interface conditions, valid to $O(\epsilon)$, are independent of the tangential velocity $\hat{v}$. These equations can now be solved in the (r, z)-plane for different values of Ca and $\hat{C}$. The unknown shape of the interface edge only enters into these equations through the normal velocity U_n and the curvature $\hat{C}$. These $O(\epsilon)$-equations for $\hat{u}$ and $\hat{w}$ are identical to the $O(\delta)$-equations for the axisymmetric problem (10), (11) and (12) discussed in §2, where

$$\epsilon\hat{C} = \frac{\epsilon}{\hat{R}} = \frac{b}{R} = \delta.$$

In fact, since the axisymmetric problem is a special case of the general problem, even the higher-order terms in the axisymmetric problem appear in (50) and (51). Since the above $O(\epsilon\hat{C})$-problem and the $O(b/R)$-axisymmetric problem are identical, the film thickness and pressure jump calculated for the axisymmetric problem are also valid for an interface edge of arbitrary shape.

6. Conclusions

In §3, we determined the perturbation solution of the axisymmetric problem for small values of Ca and $\delta = b/R$. In that problem, we assumed that the shape of the interface edge was a circle of radius R. Now, we briefly examine the perturbation solution for the more general problem (see §5) in which the interface edge has an arbitrary shape. The same expansions will still work, except that $\delta = b/R$ is replaced by $\epsilon\hat{C}$. Expansion (16*a*) is given by

$$\hat{p} = \hat{p}^0 + \epsilon\hat{C}\hat{p}^1 + Ca^{\frac{1}{3}}\hat{p}^2 + \epsilon\hat{C}\,Ca^{\frac{1}{3}}\hat{p}^3 + \ldots, \tag{54}$$

where $\hat{C}$ depends on s. If we substitute this expression into (52) and (53), we get the same results as before, except for the additional condition

$$\hat{p}_s = 0, \tag{55}$$

which follows from (53*b*). This extra condition requires that $\hat{C}$ be equal to a constant. To allow for a non-constant lateral curvature, it is necessary to further expand $\hat{C}$ in powers of $Ca^{\frac{1}{3}}$. Even in this case, all the terms will be constant until we reach the $O(Ca)$-term, at which time the velocity on the right-hand side of (53*b*) enters into the problem. This implies that lateral variations from an interface edge of constant radius R are $O(Ca)$ and not allowed until we reach these terms. It also implies that the perturbation solution in §3 gives the leading-order terms in the expansion even in the case in which the interface edge has an arbitrary shape.

The numerical results have led to boundary conditions that are valid for a much

larger range of the capillary number. These boundary conditions, which are functions of the curvature b/R and the normal velocity U_n, are valid as long as the radius of curvature R in the lateral direction is $O(a)$. If the shape of the interface edge has lateral variations of $O(b)$, as in the experiments of Nittman, Daccord & Stanley (1985), then both lateral and transverse variations of the interface are the same order and the approximations are no longer valid. In this case, it would be necessary to solve the complete three-dimensional problem in Region II.

The two new boundary conditions (6a, b), which take into account the flow in the transverse direction, are combined with the approximate equations in Region I (5a, b) to complete the two-dimensional problem. This problem can now be solved to determine the shape of the interface in the lateral direction. In previous studies, there was significant disagreement between the numerical and experimental interface-edge profiles for a given value of the capillary number. A stability analysis showed that the single steady-state fingers were unstable for all values of the capillary number. In experiments, it has been observed that the fingers are stable if the capillary number is not too large. It is hoped that interface-edge profiles and finger stability calculated with the new boundary conditions will be in closer agreement with experiments.

I wish to express my appreciation to Philip Saffman for his helpful suggestions. I would also like to thank the Department of Energy (Office of Basic Energy Sciences) DE-AMO3-76SR 00767 for providing travel funds used in association with this work.

REFERENCES

Batchelor, G. K. 1967 *An Introduction to Fluid Dynamics*. Cambridge University Press.

Bretherton, F. P. 1961 The motion of long bubbles in tubes. *J. Fluid Mech.* **10**, 166–188.

Lamb, H. 1932 *Hydrodynamics*, sixth edn. Dover.

McLean, J. W. & Saffman, P. G. 1981 The effect of surface tension on the shape of fingers in a Hele-Shaw cell. *J. Fluid Mech.* **102**, 455–469.

Nittman, J., Daccord, G. & Stanley, H. E. 1985 Fractal growth of viscous fingers: quantitative characterization of a fluid instability phenomenon. *Nature* **314**, 141–144.

Park, C. W. & Homsy, G. M. 1984 Two-phase displacement in Hele-Shaw cells: theory. *J. Fluid Mech.* **139**, 291–308.

Park, C. W. & Homsy, G. M. 1985 The instability of long fingers in Hele-Shaw flows. *Phys. Fluids* **28**, 1583–1585.

Pitts, E. 1980 Penetration of fluid into a Hele-Shaw cell: the Saffman–Taylor experiment. *J. Fluid Mech.* **97**, 53–64.

Reinelt, D. A. & Saffman, P. G. 1985 The penetration of a finger into a viscous fluid in a channel and tube. *SIAM J. Sci. Stat. Comput.* **6**, 542–561.

Saffman, P. G. & Taylor, G. I. 1958 The penetration of a fluid into a porous medium or Hele-Shaw cell containing a more viscous liquid. *Proc. R. Soc. Lond.* A **245**, 312–329.

Tabeling, P., Zocchi, G. & Libchaber, A. 1987 An experimental study of the Saffman–Taylor instability. *J. Fluid Mech.* **177**, 67–82.

Taylor, G. I. 1961 Deposition of a viscous fluid on the wall of a tube. *J. Fluid Mech.* **10**, 161–165.

Vanden-Broeck, J.-M. 1983 Fingers in a Hele-Shaw cell with surface tension. *Phys. Fluids* **26**, 2033–2034.